J. Phycol. **41,** 887–899 (2005)

DOI: 10.1111/j.1529-8817.2005.00097.x

MOLECULAR PHYLOGENY OF *STAURASTRUM* MEYEN EX RALFS AND RELATED GENERA (ZYGNEMATOPHYCEAE, STREPTOPHYTA) BASED ON CODING AND NONCODING rDNA SEQUENCE COMPARISONS[1]

Andrey A. Gontcharov[2] *and Michael Melkonian*

Botanisches Institut, Lehrstuhl I, Universität zu Köln, Gyrhofstr. 15, D-50931 Köln, Germany

Nuclear-encoded small subunit rDNA, 1506 group I intron, and internal transcribed spacer sequences were obtained from 39 strains representing five core desmid genera, *Staurastrum*, *Staurodesmus* Teil., *Cosmarium* Corda ex Ralfs, *Xanthidium* Ehr. ex Ralfs, and *Euastrum* Ehr. ex Ralfs (Desmidiaceae, Zygnematophyceae), and used individually and concatenated to assess phylogenetic relationships between putatively allied members of the family. To identify positional homology between divergent noncoding sequences, secondary structure models were generated and their reliability assessed by screening the alignment for compensating base changes. The phylogeny based on coding and noncoding sequence comparisons confidently resolved a monophyletic core of the genus *Staurastrum* but also revealed the artificial nature of the traditional genus. Twenty distinct species representing a wide range of morphotypes of *Staurastrum* formed a strongly supported generic clade that was further split into three well-resolved lineages. The phylogenetic relationships revealed within *Staurastrum* were in conflict with all previous formal or informal classifications of the genus. The genera *Staurodesmus* and *Cosmarium* were shown to be highly polyphyletic, and some morphologically similar taxa displayed high sequence divergence that exceeded generic boundaries. Apparently, the taxonomic significance of some morphological characters in *Staurastrum* and other desmid genera has been greatly overestimated.

Key index words: **1506 group I intron; ITS, Desmidiaceae; molecular phylogeny; secondary structure; SSU rDNA**

Abbreviations: **BI, Bayesian inference; BP, bootstrap percentages; CBC, compensating base change; ITS, internal transcribed spacer; ML, maximum likelihood; MP, maximum parsimony; NJ, neighbor joining; PP, posterior probability; SSU, small subunit**

The class Zygnematophyceae is the largest and most diverse group of the streptophyte green algae. A unique mode of sexual reproduction, conjugation (fusion of amoeboid nonflagellate gametes emerging from the walls of adhering vegetative cells), clearly differentiates zygnematophycean algae from other streptophytes and raises the question of the origin of this unique mode of sexual reproduction. It is possible that the loss of flagella released evolutionary constraints and enhanced speciation in an algal group that currently comprises more than 4000 described species (Hoshaw and McCourt 1988, Gerrath 1993). It is noticeable that only one family, the Desmidiaceae, which occupies a derived position within the class (McCourt et al. 2000, Gontcharov et al. 2003, 2004, Gontcharov and Melkonian 2004), contributes more than 70% of the total number of species. Within the family, species are also unevenly distributed among the 35 or so genera, with 2 of them, *Cosmarium* and *Staurastrum* (with approximately 1000 and 700 species, respectively; Gerrath 1993), being particularly species rich. Every monograph on desmid taxonomy states that these two genera are likely artificial and display transitional forms to some other genera, namely *Staurodesmus*, *Xanthidium*, and *Spinocosmarium* Prescott et Scott. These genera comprise a group of more than 2000 species that cannot be separated with confidence into "natural" entities because of the great variability of those morphological characters (shape of the cell and semicells, pattern of the cell wall ornamentation, etc.) traditionally used to distinguish species.

When describing the genera of desmids, Ralfs (1848), a pioneer of desmid taxonomy, gathered in one group unicelluar taxa with cells approximately as long as broad and included both *Cosmarium* and *Staurastrum* in this group. At that time, *Staurastrum* was regarded as distinct from other desmids because of an angular (radiate) cell shape (often with processes) in apical view. However, the characteristics of *Cosmarium* were already rather illusive: The semicells in front view were neither notched nor sinuate, and in apical view they were elliptic, circular, or cruciform (Ralfs 1848). Very soon, the great morphological diversity of new species assigned to these genera transcended the boundaries established by Ralfs and called for their reevaluation. The most common way desmid specialists dealt with this situation was to separate a group of taxa with pronounced morphological features (often

[1]Received 12 September 2004. Accepted 25 April 2005.
[2]Author for correspondence and present address: Institute of Biology and Soil Science, 690022, Vladivostok-22, Russia. E-mail: gontcharov@ibss.dvo.ru.

without knowledge about the stability or functional significance of those features) into a new smaller taxon (genus or subgenus). Basically, none of these entities earned the universal approval of the specialists because of the growing number of transitional taxa (for a brief history of the taxonomy of the two genera, see Prescott et al. 1981, 1982, Croasdale et al. 1994). Thus, neither in *Cosmarium* nor in *Staurastrum* has the concept of a genus changed significantly over the last 150 years, and the need for taxonomic revisions of these taxa has been raised frequently (Brook 1981, Prescott et al. 1981, 1982, Gerrath 1993).

Perhaps the only widely accepted rearrangement of the taxa has been that of the Swedish phycologist Teiling, who established the genus *Staurodesmus* (Teiling 1948) by merging triradiate species of *Staurastrum* and biradiate species of *Arthrodesmus* Ehr. ex Ralfs in which each angle of the cell bears a single spine as the only decoration of the cell wall. Another of Teiling's new taxa was the genus *Actinotaenium* Teil. (Teiling 1954), which includes those former members of *Cosmarium* with circular cell outlines in apical view and only a very small shallow median cell constriction. The most recent attempt to split *Staurastrum* into four genera based on numerical analyses of morphological features (Palamar-Mordvintceva 1976, 1982) was acknowledged as sound (Prescott et al. 1982) but has not been used in the latest taxonomic treatments of the family (Coesel 1997, Lenzenweger 1997, Brook 2002, Gerrath 2003).

In a recent study, the phylogeny of the Desmidiaceae and the question of the monophyly of its genera were addressed with molecular tools (Gontcharov et al. 2003). None of the genera mentioned above (*Spinocosmarium* was not analyzed) was resolved as monophyletic in nuclear-encoded small subunit (SSU) rDNA sequence comparisons. However, there was an indication that at least in some cases this result could be attributed to either insufficient resolution of the SSU rRNA gene or unequal evolutionary rates among sequences. In *Staurastrum*, eight of nine species/strains analyzed formed a cluster (without bootstrap support) and one taxon, *S. tumidum*, showed an affinity to members of the genus *Xanthidium* (Gontcharov et al. 2003). In contrast, six *Cosmarium* sequences were broadly distributed in the tree associated with representatives of several other genera of the Desmidiaceae. Sequence divergence was relatively low among *Staurastrum* species, and this may have contributed to the lack of support for their monophyly, whereas in *Cosmarium* two of the six species analyzed displayed long branches that could have disrupted the monophyly of *Cosmarium* due to long branch attractions. Among four analyzed members of the genus *Staurodesmus*, only one species was fast evolving, but the remaining species/strains did not show any affinity to each other.

To evaluate the monophyletic core of the genera forming the bulk of the taxa in the family Desmidiaceae and to test phylogenetic hypotheses raised by the previous study (Gontcharov et al. 2003), we extended the taxon sampling in *Staurastrum* and *Staurodesmus* and increased the data set, adding new molecular markers. We generated an alignment comprising coding (SSU rDNA, 5.8S) and noncoding (1506 group I intron, internal transcribed spacer [ITS] regions 1 and 2) sequences of 38 taxa (39 strains) of the family Desmidiaceae and analyzed these partitions individually and in concatenation using different phylogenetic methods.

MATERIALS AND METHODS

Cultures. Thirty-nine strains of Desmidiaceae used for this study were obtained from different sources (Table 1) and grown in modified WARIS-H culture medium (McFadden and Melkonian 1986) at 20° C with a photon fluence rate of 40 μmol photons $\cdot m^{-2} \cdot s^{-1}$ in a 14:10-h light:dark cycle. In sampling the genus *Staurastrum* (23 species, 24 strains), we aimed to cover the whole range of its morphological diversity and to analyze representatives for most of its sections as established by West and West (1912) as well as for the genera separated from *Staurastrum* by Palamar-Mordvintceva (1976, 1982). To assess the variability of noncoding sequences at the species level, we included two strains of a morphologically distinct species, *S. arctiscon*, originating from Japan (CCAC 0116) and North America (SVCK 152), respectively. In *Staurodesmus* (nine species), taxa that are triangular (five species) or elliptical in apical view (four species) are represented. Given the considerable SSU rDNA sequence diversity previously found in *Cosmarium* (Gontcharov et al. 2003), we restricted our taxon sampling in this genus to two morphologically similar and likely closely related species, *C. contractum* and *C. depressum*, and two additional morphologically distinct taxa. *Xanthidium armatum* was included as a putative sister taxon to *Staurastrum tumidum* (Meindl 1986, Höftberger and Meindl 1993, Gontcharov et al. 2003).

DNA extraction, amplification, and sequencing. After mild ultrasonication to remove mucilage (Surek and Sengbusch 1981), total genomic DNA was extracted using the DNeasy Plant Mini Kit (Qiagen, Hilden, Germany). The SSU rDNA, 1506 group I intron, and ITS regions were amplified by PCR using published protocols and 5′-biotinylated PCR primers (Marin et al. 1998). PCR products were purified with the Dynabeads M-280 system (Dynal Biotech, Oslo, Norway) and used for bidirectional sequencing reactions (for protocols, see Hoef-Emden et al. 2002). Gels were run on an IR^2 DNA sequencer (LI-COR Inc., Lincoln, NE, USA).

Sequence alignments and tree reconstructions. Sequences were manually aligned using the SeaView program (Galtier et al. 1996). For coding regions of the SSU rDNA of the Zygnematophyceae, the alignment was guided by primary and secondary structure conservation (Wuyts et al. 2000, 2001; http://oberon.rug.ac.be:8080/rRNA/). The alignment of the 1506 group I introns (Bhattacharya et al. 1994) and their secondary structures (Bhattacharya et al. 1996) were used to guide incorporation of new intron sequences. Alignments are available upon request or from GenBank (accession numbers ALIGN_000867 and ALIGN_000868). To elucidate the folding pattern of secondary structure elements of the introns, the web mfold server (version 3.1; Zuker 2003) was used. ITS secondary structures were generated as described in Mai and Coleman (1997). After structural elements were identified in the transcripts, the alignment was refined and screened for compensating base changes (CBCs).

Phylogenetic trees were inferred with maximum likelihood (ML), distance (neighbor joining [NJ]), and maximum parsimony (MP) optimality criteria using PAUP 4.0b10 (Swofford 2002) and Bayesian inference (BI) using MrBayes v3.0b3 (Huelsenbeck and Ronquist 2001). Evolutionary models (for

TABLE 1. Origin and taxonomic designation of strains and corresponding EMBL/GenBank accession numbers of the sequences used.

Taxon	Strain	GenBank accession numbers
Cosmarium contractum Kirchn.	SVCK396	AJ428112, **AJ829661**
C. depressum (Näg). Lund.		**AJ829664**
C. dilatatum Lütkem. et Grönbl.	SVCK463	**AJ829665**
C. isthmium W. West var. *hibernica* W. West	SVCK229	AJ428116, **AJ829663**
Euastrum pectinatum (Bréb.) ex Bréb. var. *rostratum* (Tayl.) W. Krieg.	SVCK203	**AJ829662**
Staurastrum alternans Bréb. in Ralfs (= *Cosmoastrum alternans* (Bréb. in Ralfs) Pal.-Mordv.) **Sect. D**	M2118	**AJ829638**
S. arctiscon (Ehr. ex Ralfs) Lund **Sect. J**	SVCK152	**AJ829642**
S. arctiscon	CCAC 0116	AJ428105, **AJ829641**
S. brachiatum Ralfs **Sect. H**	SVCK222	**AJ829650**
S. brachycerum Bréb. **Sect. I**	M2218	**AJ829647**
S. brebissonii W. Arch. in Pritch. (= *Cosmoastrum brebissonii* (W. Arch. in Pritch.) Pal.-Mordv.) **Sect. E**	SVCK278	**AJ829634**
S. capitulum Bréb. in Ralfs (= *Cosmoastrum capitulum* (Bréb.) Pal.-Mordv.) **Sect. A**	ASW07233	**AJ829636**
S. dispar Bréb. (= *Cosmoastrum dispar* (Bréb.) Pal.-Mordv.) **Sect. D**	M2117	**AJ829631**
S. hirsutum (Ehr.) Bréb. in Ralfs (= *Cosmoastrum hirsutum* (Ehr.) Pal.-Mordv.) **Sect. E**	M0752	X74752, **AJ829633**
S. lunatum Ralfs (= *Raphidiastrum lunatum* (Ralfs) Pal.-Mordv.) **Sect. E**	SVCK15	AJ428106, **AJ829640**
S. maamense Arch. (= *Cosmoastrum maamense* (Arch.) Pal.-Mordv.) **Sect. G**	SVCK377	**AJ829646**
S. majusculum Wolle (= *S. minnesotense* var. *majusculum* (Wolle) Scott et Grönbl., *Std. majusculus* (Wolle) Bourr.) **Sect. E**	SVCK330	**AJ829635**
S. margaritaceum (Ehr.) Menegh. ex Ralfs **Sect. I**	M2220	**AJ829649**
S. monticulosum (Bréb.) Bréb. ex Ralfs (= *Raphidiastrum monticulosum* (Bréb.) Pal.-Mordv.) **Sect. J**	ASW07238	**AJ829639**
S. ophiura Lund. **Sect. I**	M1027	AJ428104, **AJ829643**
S. orbiculare (Ehr.) ex Ralfs (= *Cosmoastrum orbiculare* (Ehr.) Pal.-Mordv.) **Sect. C**	M2217	**AJ829660**
S. paradoxum Meyen ex Ralfs **Sect. I**	M1129	**AJ829629**
S. polymorphum Bréb. ex Ralfs **Sect. I**	SVCK119	**AJ829632**
S. pyramidatum W. West (= *Cosmoastrum pyramidatum* (W. West) Pal.-Mordv.) **Sect. E**	SVCK131	**AJ829637**
S. sebaldi Reinsch **Sect. H**	M1133	**AJ829630**
S. simonyi Heimerl (= *Raphidiastrum simonyi* (Heimerl) Pal.-Mordv.) **Sect. F**	M2219	**AJ829645**
S. spongiosum Bréb. *ex* Ralfs **Sect. G**	ASW07228	**AJ829648**
S. subavicula (W. West) W. et G.S. West **Sect. J**	M0754	AJ428107, **AJ829644**
S. tumidum Bréb. ex Ralfs (= *Pleurenterium tumidum* (Bréb.) Wille, *Staurodesmus tumidus* (Bréb.) Teil.) **Sect. C**	SVCK85	AJ428108, **AJ829666**
Staurodesmus bieneanus (Rabenh.) Florin (= *Std. spetsbergensis* (Nordst.) Teil.. *Staurastrum bieneanum* Rabenh.) **Sect. C**	M1130	**AJ829659**
Std. bulnheimii (Racib.) Round et Brook (= *Arthrodesmus bulnheimii* Racib.)	SVCK84	AJ428111, **AJ829657**
Std convergens (Ehr. ex Ralfs) Lillier. (= *Arthrodesmus convergens* Ehr. ex Ralfs	CCAC0120	AJ428102, **AJ829651**
Std mamillatus (Nordst.) Teil. (= *Staurastrum mamillatum* Nordst.)	M2099	**AJ829656**
Std. mucronatus (Ralfs ex Bréb.) Croasd. (= *Staurastrum mucronatus* Ralfs ex Bréb.)	M1394	AJ428103, **AJ829658**
Std. omearii (Arch.) Thom. (= *Staurastrum omearii* Arch.)	M0751	**AJ829655**
Std. subulatus (Kütz.) Thom. var. *subaequalis* (W. et G.S. West) Thom. (= *Arthrodesmus subulatus* Kütz. var. *subaequalis* W. et G.S. West)	SVCK106	**AJ829652**
Std. triangularis (Lagerh.)Teil. (= *Arthrodesmus triangularis* Lagerh.)	SVCK280	**AJ829654**
Std. validus (W. et G.S. West) Scott et Grönbl. (= *Arthrodesmus validus* W. et G.S. West)	SVCK457	**AJ829653**
Xanthidium armatum (Bréb.) Rabenh. ex Ralfs	ASW07059	AJ428094, **AJ829667**

Sequences determined for this study are indicated by accession numbers in bold type. For the species of the genera *Staurastrum* and *Staurodesmus*, synonymy is provided. The corresponding sections (West and West 1912) are indicated for *Staurastrum* taxa. Sources of the strains: ASW, Algensammlung Wien (Kusel-Fetzmann and Schagerl 1992); CCAC, Culture Collection of Algae at the University of Cologne (Surek and Melkonian 2004; http://www.ccac.uni-koeln.de); M, Research Culture Collection Melkonian (University of Cologne, Germany); SVCK, Sammlung von Conjugaten-Kulturen (http://www.biologie.uni-hamburg.de/b-online/d44_1/44_1.htm). The strains not held by public collections are available upon request.

TABLE 2. Evolutionary models, log likelihood values (–lnL), and settings identified by Modeltest (Posada and Crandall 1998) for different data sets used for Figures 4 and 5 and for special analyses.

	SSU rDNA (Fig. 4)	1506 group I intron	ITS1	ITS2	Combined (Fig. 5)	*Staurastrum* 21 strain
	TrN + I + Γ	TrNef + Γ	TrN + Γ	K80 + Γ	TrN + I + Γ	TrN + I + Γ
–lnL						
I	0.7743	0	0	0	0.5956	0.6494
Γ	0.6719	0.3886	0.5883	0.6174	0.4715	0.5281
Base frequencies						
A	0.2636	Equal	0.2561	Equal	0.2667	0.2517
C	0.1995	Equal	0.2752	Equal	0.2251	0.2227
G	0.2615	Equal	0.1814	Equal	0.2417	0.2512
T	0.2754	Equal	0.2873	Equal	0.2665	0.2744
G + C	0.461	0.5	0.4556	0.5	0.4668	0.4739
Rate matrix ([G ↔ T = 1.00])						
[A ↔ C]	1.0000	1.0000	1.0000	Equal	1.0000	1.0000
[A ↔ G]	1.6124	3.5504	3.0061	Equal	2.5481	2.7798
[A ↔ T]	1.0000	1.0000	1.0000	Equal	1.0000	1.0000
[C ↔ G]	1.0000	1.0000	1.0000	Equal	1.0000	1.0000
[C ↔ T]	7.8376	6.7699	3.2241	Equal	4.3277	5.1106
Aligned nt	1747	263	270	149	2633	2914
Constant nt	1569	103	62	27	1902	2331
MP informative	80	126	168	102	504	391
MP uninformative	98	34	40	20	227	192

ML and NJ analyses) for the different data sets were selected via hierarchical likelihood ratio tests using Modeltest 3.04 (Posada and Crandall 1998). The models selected and model parameters are summarized in Table 2. Distances for NJ analyses were calculated by ML. The ML and MP analyses used heuristic searches with a branch-swapping algorithm (tree bisection-reconnection). In BI, the Markov chains were run for one million generations sampling every 100 generations for a total of 10,000 samples. The first 500 samples were discarded as "burn-in" and the remaining samples were analyzed using the "sumt" command in MrBayes. The robustness of the trees was estimated by bootstrap percentages (BP) (Felsenstein 1985) using 1000 (NJ) or 100 (ML and MP) replications and by posterior probabilities (PP) in BI. Bootstrap percentages $<50\%$ and PP <0.90 were not taken into account. In MP, the stepwise addition option (10 heuristic searches with random taxon input order) was used for each bootstrap replicate. The ML bootstrap used a single heuristic search (starting tree via stepwise addition) per replicate.

RESULTS

Noncoding 1506 group I intron alignment. As expected, the SSU rDNA coding region of all species studied contained the well-known 1506 group I intron at the 3′ end. Although no prominent indels were revealed in the intron sequences, their length varied from 363 nt in *Cosmarium depressum* to 467 nt in *Staurodesmus mucronatus*. On average, an intron was 413 nt long (SD, ± 24) with a mean G + C content of 55.3% (SD, ± 0.05). The lowest G + C value was recorded in *Euastrum pectinatum* (44.6%) and the highest (66.6%) in *Staurodesmus bulnheimii*.

The predicted secondary structure of the intron basically agreed with that of *Gonatozygon* (*Genicularia*) *spirotaenium* de Bary except for the lack of the P2* helix typical for other representatives of the class (Bhattacharya et al. 1996). The desmid taxa analyzed showed significant sequence conservation in the catalytic core of the intron (elements P, Q, R, and S) (Cech 1988, Michel and Westhof 1990). The segments P3, P4, P7, J3/4, J6/7, and J8/7 were almost invariant among the 38 taxa and served as benchmarks for the alignment, whereas the P1, P2, P5, P6, P8, and P9 stem-loop elements accounted for the observed variation in primary sequence and sequence length. In these stems, sequence conservation was limited to the basal 4–5 bp (not shown). Usually, members of the clades (see below) had introns of the same or very similar lengths and shared the same characteristic indels. For the global analyses, 263 nt were included in the data set, whereas for the less diverse *Staurastrum* sequences, the alignment was extended to 320 unambiguously aligned positions.

ITS1 alignment and secondary structure. The ITS1 was somewhat shorter than the 1506 group I intron, ranging from 329 nt in *Staurodesmus omaerii* to 415 nt in *Staurastrum tumidum* with a mean length of 370 nt (SD, ± 17.3). In general, the lengths of the desmid ITS1 sequences were less variable than the lengths of the 1506 intron and in most taxa ranged from 355 to 375 nt with a G + C content of 55.8% (SD, ± 0.05). Only in two taxa, *Euastrum pectinatum* and *Staurastrum alternans*, the G + C content in the ITS1 sequences was less than 50% (45% and 48.4%, respectively). It should be noted that in all species studied, the base frequencies were unevenly distributed over the length of the ITS1 with the 3′ part being notably A + T rich.

The primary sequence of the ITS1 varied considerably in the family Desmidiaceae and only 62 nt (∼ 16%) were universally conserved among the 38 taxa studied. Identification of ITS1 positional homology was not possible without considering the secondary structure that we obtained for all sequences. The thermodynamically predicted model of the desmidiacean ITS1 transcript identified six stem-loop do-

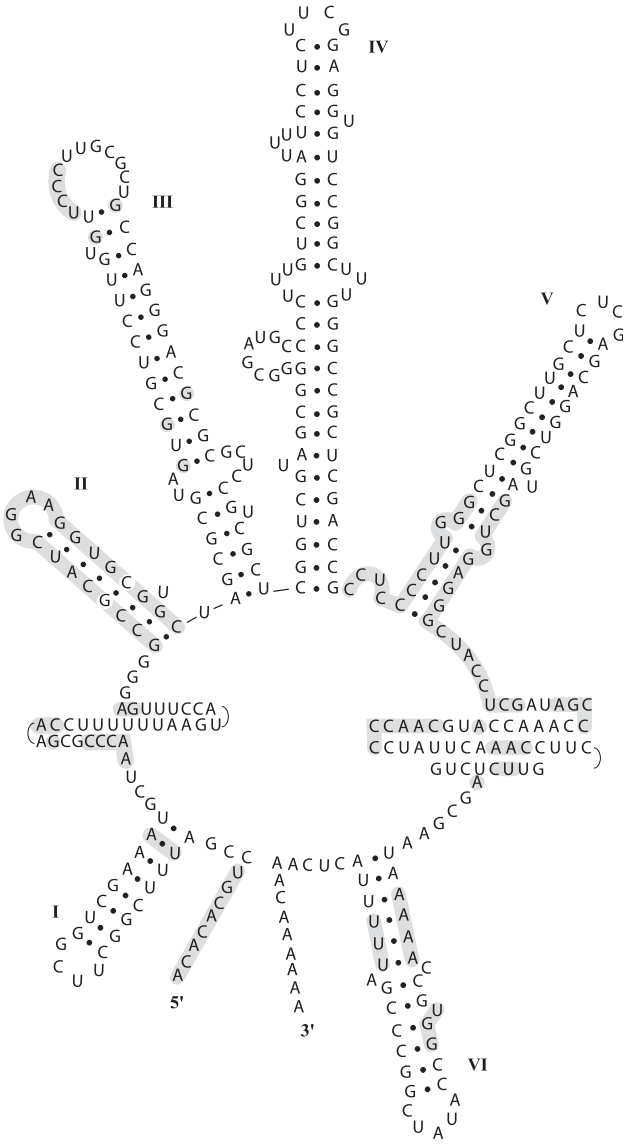

FIG. 1. Putative secondary structure model of the ITS1 transcript of *Staurastrum lunatum* generated with thermodynamic-based RNA folding algorithms (Mathews et al. 1999) and supported by CBCs and hemi-CBCs, which preserve base pairing in helices. The six domains are labeled I–VI. Nucleotide positions absolutely conserved among 21 *Staurastrum* sequences forming the generic clade (STAUR + SEB; see Results) are in bold. Nucleotides conserved in 90% of the 39 desmid sequences analyzed are highlighted (shaded background).

mains (termed I–IV; Fig. 1). Approximately 50% of the nucleotides were involved in the formation of the stem-loops. The longest single-stranded CA-rich region (Goertzen et al. 2003) extending between stems V and VI had some well-conserved motifs that were easily identifiable among the taxa, but its complete alignment was not possible due to the length variations among sequences. The second extensive nonpairing region separating stems I and II also had several conserved motifs (Fig. 1). Stem-loop II was the most conserved of all stem-loops both with respect to length (8 bp) and primary sequence. This stem was capped with an invariant GGAA tetraloop that corresponds to the GNRA motif of hairpin loops typical for RNA molecules (Woese et al. 1990). Another region of ITS1 primary sequence conservation is the base of stem V with its universally conserved first 8 bp (including a characteristic purine-purine mismatch at the position 6) and invariant flanking spacers, intercalated between helix IV and the CA-rich single-stranded region. The long hairpin stems III and particularly IV had the lowest sequence conservation, although their secondary structure with characteristic loops in the stem regions was maintained among the sequences analyzed (Fig. 1).

The amount of sequence diversity and the consistency of the predicted secondary structures across several desmid genera suggested that CBCs in the stem regions must be frequent to maintain functionality in these structures. Indeed, examination of the secondary structure-based alignment revealed numerous compensating nucleotide changes supporting our predictions (Fig. 2). Within the same clade (see below) one-sided (hemi-) CBCs could be found more often but with increasing phylogenetic divergence between the sequences, two-sided (compensatory) substitutions become more frequent. The frequency of nucleotide changes generally increased toward the distal part of the helices, but the terminal one or two base pairs were again well conserved. An alignment based on the predicted secondary structure resulted in 270 characters available for the phylogenetic analyses of 39 sequences and 357 characters for the refined analyses of the *Staurastrum* clade (21 sequence; see below).

ITS2 alignment and secondary structure. The shortest ITS2 sequence was found in *Cosmarium depressum* (252 nt), a species that also had the second shortest ITS1 sequence (342 nt). The same trend was seen in *Staurastrum tumidum*, which has the longest ITS2 (352 nt) and ITS1 sequences. In the taxa studied, the ITS2 was generally shorter than the ITS1 and more variable in length (307 ± 24 nt) and primary sequence (only 30 nt were universally conserved among 39 sequences). The low number of conserved position was caused by the presence of a few divergent species in the data set, and at a conservation level of 90% the number of conserved positions more than doubled (71 nt). However, even then only two relatively long strings of conserved positions were observed, one near the start of the ITS2 (15 nt) and the second in its central part (17 nt). Numerous indels hampered straightforward sequence alignment.

Folding of sequences produced the ITS2 secondary structure model presented in Figure 3. The ITS2 in the Desmidiaceae, as in many eukaryotes, displayed four stem-loop regions (I, II, III, and IV). Helix III (with an additional short arm near the 3′ end) was the longest and helix IV the most variable in length of the four stem-loops. Conserved motifs were unevenly distributed over the spacer elements and included both stems and single-stranded spacers (Fig. 3). The basal

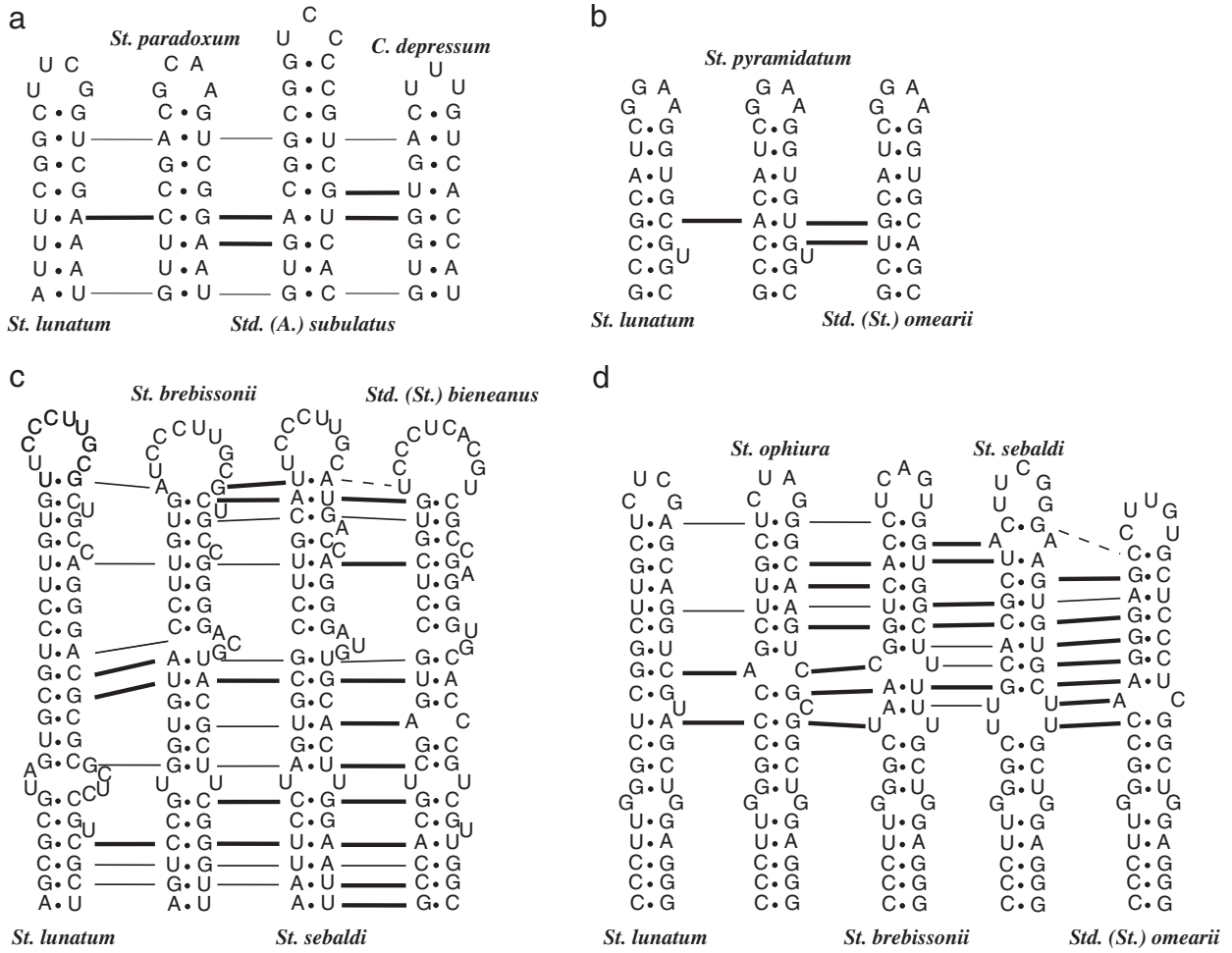

FIG. 2. Examples of CBCs (solid line) and hemi-CBC (thin line) in helices I (a), II (b), IV (c), and IV (d) of the ITS1 transcript from representative taxa. *Staurastrum lunatum* was selected as a reference species. The order of taxa reflects their decreasing relatedness as shown by phylogenetic analyses (Figs. 4 and 5). Dashed lines denote uncertain homology between positions.

parts of the first two helices, I and II, and their flanking spacers exhibited a high degree of primary sequence conservation, and the first nucleotide pairs of the stem regions were invariant across the data set, whereas the divergence increased toward their distal parts. Stem II revealed a pyrimidine mismatch (C-C in most taxa; arrows in Fig. 3) at position 5 that was previously reported in many distantly related groups of organisms (Mai and Coleman 1997, Joseph et al. 1999, Coleman and Vacquier 2002, Goertzen et al. 2003). In helix III, sequence conservation increased toward its distal part where the longest string of invariant nucleotides (including a highly conserved UGG motif) (Coleman 2003, Goertzen et al. 2003) was located (Fig. 3). An optional arm at the end of the 3′ side of the helix was observed at the same position in most of the taxa. Only four species, *Cosmarium contractum*, *C. dilatatum*, *Euastrum pectinatum*, and *Staurodesmus mamillatus*, lacked this 5-to 7-bp-long helix. The region of the highest sequence variability in the ITS2 referred to stem IV and the following terminal spacer (Fig. 3). The length of this stem varied greatly, and no motifs common to all taxa were found. Because of its greater sequence variation, the ITS2 alignment contributed only 149 nt to the global phylogenetic analyses and 282 nt to the phylogenetic analyses of the *Staurastrum* clade.

SSU rDNA phylogeny. The selected model for the SSU rDNA data set was TrN with gamma shape-parameter (Γ) and proportion of invariable sites (I). The value of one substitution rate category, C ↔ T, was considerably elevated (7.8376) compared with those of other categories (Table 2).

Unrooted ML analyses of a data set that included 38 taxa of Desmidiaceae and 1747 nt produced the tree presented in Figure 4. Only a few clades obtained significant bootstrap support in this phylogeny, and relationships between the clades remained mostly unresolved. The major moderately supported clade (65%–76% BP, 0.99 PP) comprised 20 of 24 *Staurastrum* sequences analyzed (clade STAUR; Fig. 4) with one more species of the genus, *S. sebaldi*, being a sister to this assemblage, however, without BP and PP support. Of the three remaining *Staurastrum* species, *S. brachiatum* showed no affinity to any other taxon, where-

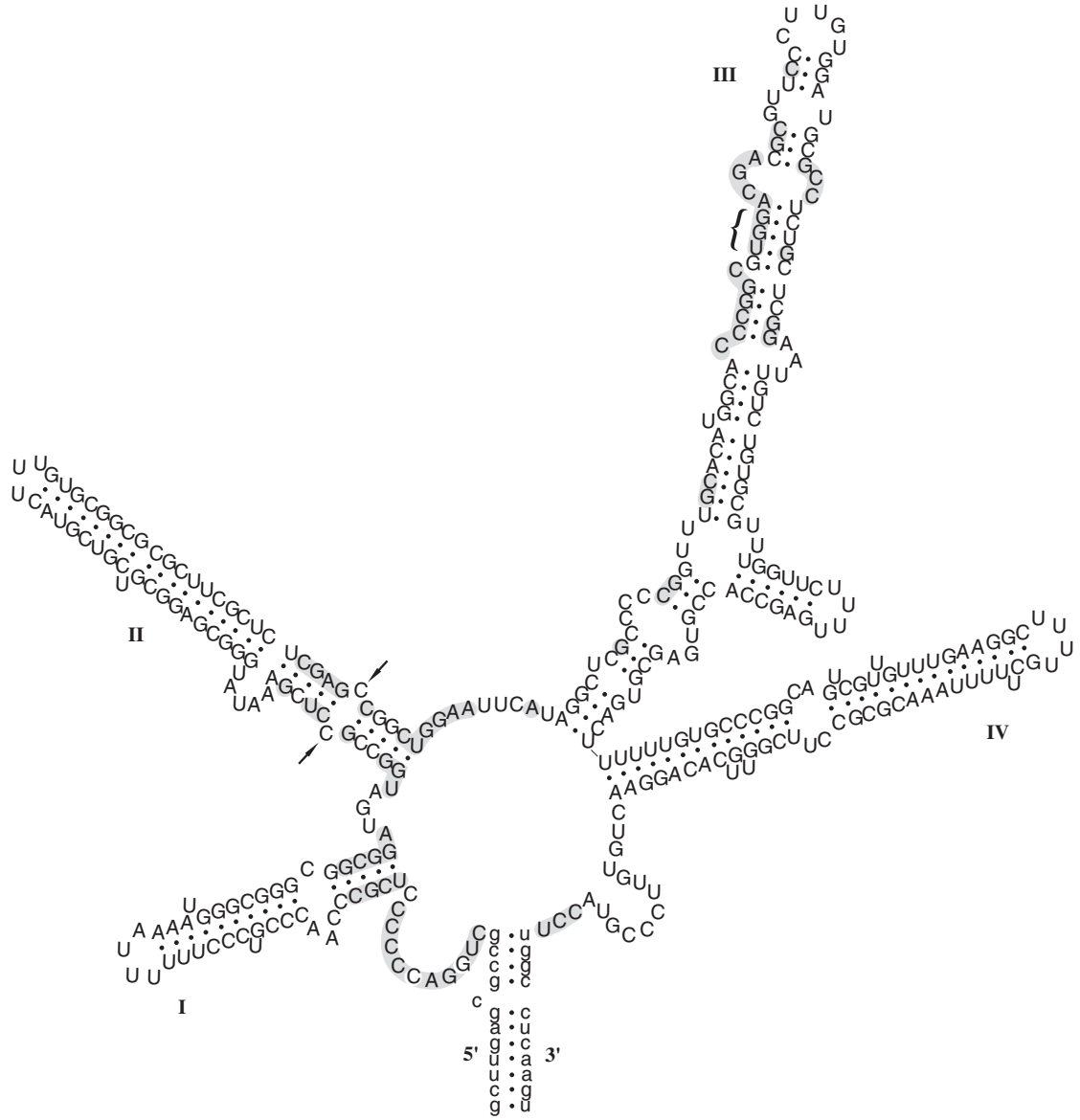

FIG. 3. Putative secondary structure model of the ITS2 transcript of *Staurastrum lunatum* generated with thermodynamic-based RNA folding algorithms (Mathews et al. 1999). The four helical domains are labeled I–IV. The pyrimidine-pyrimidine bulge in helix II is marked with arrows, and the UGG motif universal in the Streptophyta is labeled with a bracket. Nucleotide positions that are absolutely conserved among 21 *Staurastrum* sequences forming the generic clade (STAUR + SEB) are in bold. Nucleotides conserved in 90% of the 39 desmid sequences analyzed are highlighted (shaded background). The nucleotides at the 3′ end of the 5.8 S and the 5′ end of the LSU rRNA are italicized.

as *S. tumidum* was positioned as a sister to *Xanthidium armatum*, albeit with low support (50%–65% BP, 0.95 PP). Finally, *Staurastrum orbiculare* was significantly nested within members of the genus *Staurodesmus* (STD 2 clade, 99%–100% BP, 1.00 PP). The STAUR clade was further split into two very weakly supported subclades, with 11 and 9 strains, respectively. Only a few internal branches within the STAUR subclades attained any support, except for a robust group of three taxa, *S. polymorphum*, *S. paradoxum*, and *S. dispar* (100% BP, 1.00 PP). Another less-well supported association comprises *S. pyramidatum*, *S. hirsutum*, and *S. brebissonii*.

The genus *Staurodesmus*, represented by nine sequences, was not monophyletic with its members being distributed into three strongly supported clades (94%–100% BP, 1.00 PP) each with relatively long branches (STD 1, STD 2, and ARTHR; Fig. 4) and two individual branches, *Staurodesmus mamillatus* and *S. bulnheimii*, which showed no affinity to each other or to other taxa. Two of these clades, STD 2 and ARTHR, included members of other genera as well, *Staurastrum* and *Cosmarium*, respectively. The basal position of *Staurodesmus mucronatus* in the STD 2 clade was firmly established, whereas the branching pattern within the ARTHR

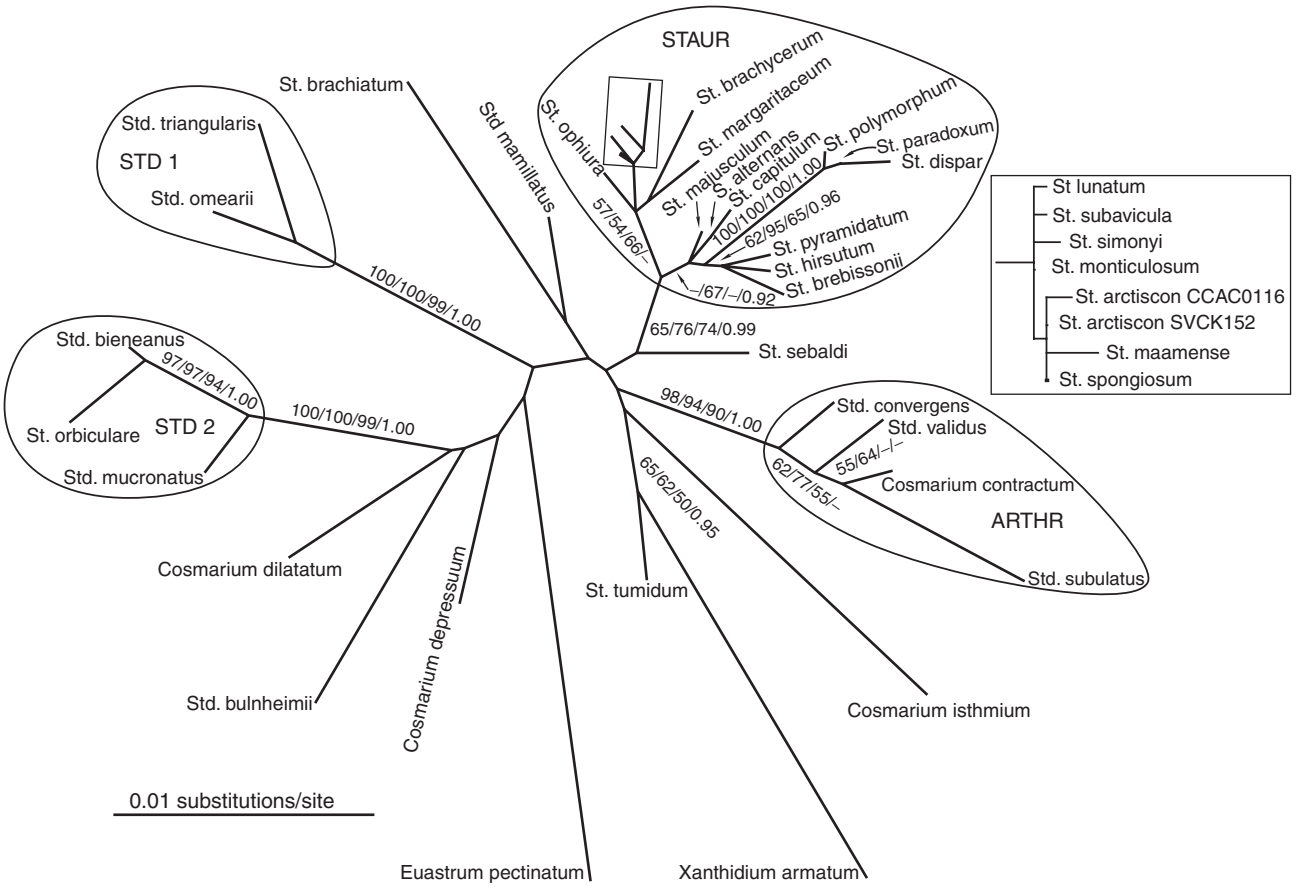

FIG. 4. Unrooted phylogenetic tree showing relationships between representatives of several putatively related desmid genera (Desmidiaceae, Zygnematophyceae) based on comparisons of 39 SSU rDNA sequences (38 species; 1747 aligned positions). The topology was inferred by maximum likelihood (TrN + I + Γ, for model parameters, see Table 2). Nodes are characterized by bootstrap percentages (BP ≥ 50%) and Bayesian posterior probabilities (PP ≥ 0.9): ML/NJ (TrN + I + Γ)/MP/BI. For abbreviation of clade names, see Results.

clade attained only weak BP and PP support (Fig. 4). Three taxa, *Cosmarium isthmium*, *Euastrum pectinatum*, and *Xanthidium armatum*, revealed long branches, which may have affected the significance of some other branches; however, they were not artificially attracted (Fig. 4).

Molecular phylogenies based on noncoding regions of the rDNA operon. For the noncoding regions of the rDNA operon (i.e. the 1506 group I intron, ITS1, and ITS2), different evolutionary models were selected (Table 2). Compared with the SSU rDNA, the larger sequence variability resulted in the exclusion of the proportion of invariable sites from the models selected for these partitions (Table 2). The relatively low values of the gamma shape-parameter (Γ) identified for the intron and the spacers (0.3886 to 0.6174) reflected an uneven distribution of substitutions across these data sets. The substitution rate matrixes were particularly biased between the partitions. Two substitution categories (C ↔ T and A ↔ G) were generally elevated; however, they had distinct patterns in the different alignments (Table 2).

Despite the differences in the evolutionary models and their parameters, the phylogenies resulting from the three different noncoding regions were similar to each other and to that obtained for the SSU rRNA gene (not shown). The ITS2 topology was the least informative regarding STAUR (no support) and its subclades (only one was supported), whereas the clades STD 1, STD 2, and particularly ARTHR attained moderate to high bootstrap support (>70% BP; not shown). In the intron tree, STAUR was also not supported; however, its internal topology was much better resolved than in the ITS2 tree (not shown). This data set again strongly supported three independent *Staurodesmus* clades and in addition revealed a weakly supported association of *Cosmarium depressum* and *C. dilatatum*. The intron and ITS1 alignments were nearly equal in length; however, the latter had a significantly larger number of informative positions (168 compared with 126 for the intron data set) that resulted in better resolution. The ITS1 data set favored the monophyly of the *Staurastrum* cluster that now also included *S. sebaldi* (>95% BP). Most internal branches of STAUR were also resolved with moderate to high BP and PP support in the ITS1 tree (results not shown) as were the three *Staurodesmus* clades (STD 1, STD 2, and ARTHR; 77%–100% BP). The putative sister group

relationship between *Xanthidium armatum* and *Staurastrum tumidum* (Fig. 4) received no support in phylogenies based on the noncoding partitions. The three long-branch taxa in the SSU rDNA analyses (*C. isthmium*, *E. pectinatum*, and *X. armatum*) also displayed the longest branches of the trees derived from the noncoding regions of the rDNA operon.

Combined analyses of coding and noncoding rDNA sequences. The concatenated data set consisted of 2633 nt, and the predicted model for it was TrN with gamma shape (Γ) and proportion of invariable sites (I). Model parameters were averaged between those for coding (SSU rDNA) and noncoding (1506 group I intron, ITS1, and ITS2) partitions with respect to the value of C ↔ T and A ↔ G categories (Table 2; the 5.8 S rDNA data set [154 nt] contained only nine MP-informative positions; therefore, no separate analyses were performed using this gene). The tree topology was very similar to that obtained with the SSU rDNA sequences and resolved the same clades, however, with much better support (Fig. 5). The split between STAUR plus *S. sebaldi* (STAUR + SEB, Fig. 5) and the remaining sequences was strongly supported by all methods of analyses (95%–100% BP, 1.00 PP), and the major internal branches within STAUR + SEB obtained BP and PP support (Fig. 5). In contrast, the phylogenetic relationships between taxa and clades outside STAUR + SEB remained largely unresolved. The *Staurastrum* taxa excluded from STAUR + SEB were either grouped with representatives of other genera (*S. tumidum* with *Xanthidium armatum* [>88% BP, 1.00 PP] and *S. orbiculare* with *Staurodesmus bieneanus*/*S. mucronatus* [100% BP, 1.00 PP; STD 2]) or comprised an individual branch (*Staurastrum brachiatum*). Similarly, the genera *Cosmarium* and *Staurodesmus* were polyphyletic, and the two morphologically similar species of *Cosmarium*, *C. depressum* and *C. contractum*, were quite distant from each

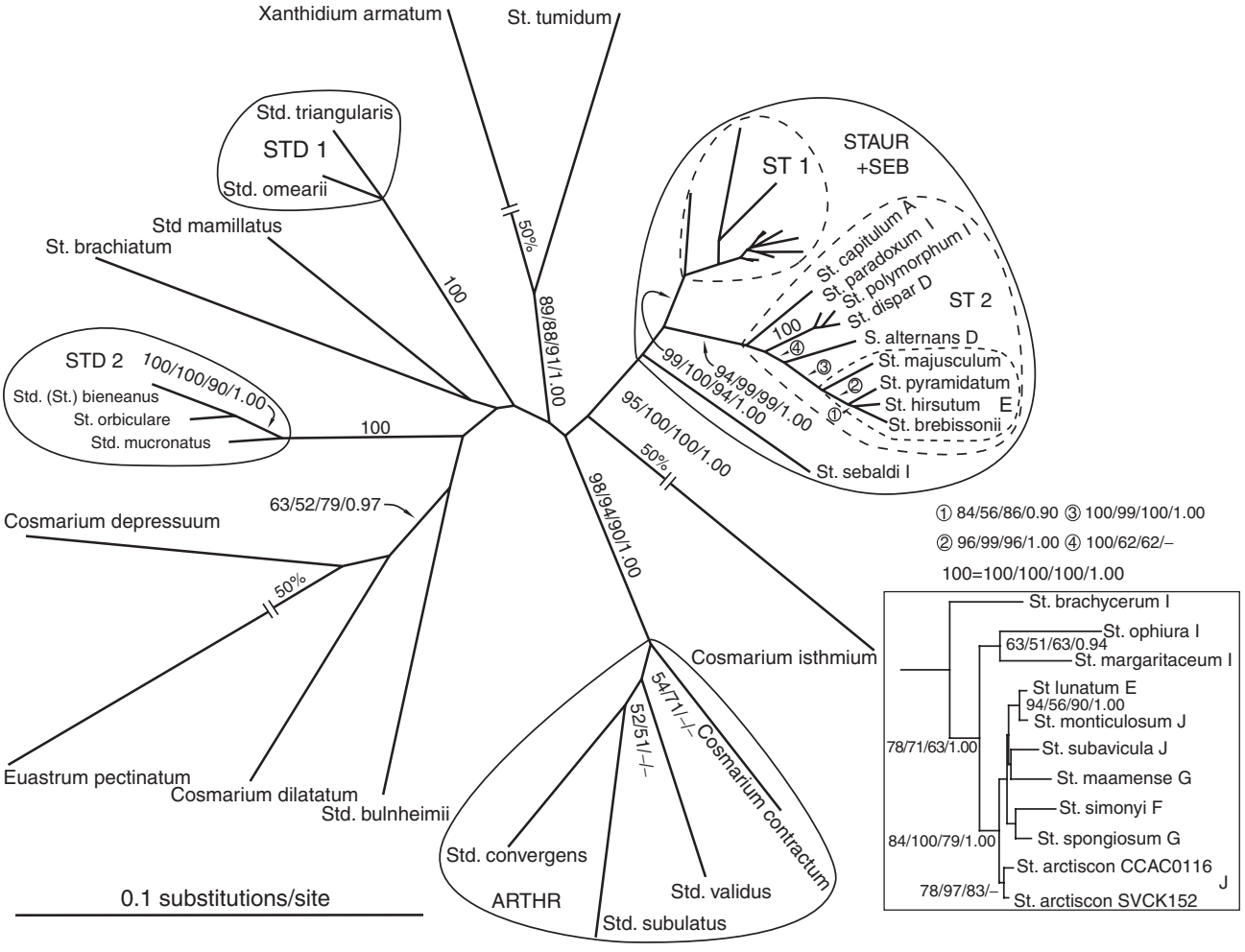

FIG. 5. Unrooted phylogenetic tree of 39 strains (38 species) representing five traditional desmid (Desmidiaceae, Zygnematophyceae) genera based on comparisons of concatenated coding (SSU rDNA and 5.8S) and noncoding (1506 group I intron, ITS1, and ITS2) rDNA sequences (2633 aligned positions). The tree shown was constructed with ML (TrN + I + Γ, for model parameters, see Table 2). BP ≥ 50% for ML/NJ (TrN + I + Γ)/MP and PP ≥ 0.9 (Bayesian inference) values are given for the nodes; long branches are graphically reduced to 50%. For abbreviation of clade names, see Results. Sections of *Staurastrum* (STAUR + SEB) according to West and West (1912) are labeled by capital letters (A, D, E, F, G, I, and J).

other (Fig. 5). In general, the sequences outside STAUR + SEB were all characterized by relatively long individual branches.

Within STAUR + SEB, most of the taxa were arranged in two strongly supported derived subclades (ST 1 and ST 2), and *S. sebaldi* formed the basal divergence (Fig. 5). The larger subclade, ST 1, consisted of 11 sequences (10 species) of taxa with different morphology representing five sections of West and West (1912). Three divergent sequences (*S. brachycerum, S. ophiura*, and *S. margaritaceum*) occupied basal positions in this subclade (63%–100% BP, 1.00 PP), whereas eight very similar sequences representing seven morphologically distinct species formed a well-supported crown group (>79% BP, 1.00 PP; Fig. 5) within this subclade. The subclade ST 2 was somewhat better structured, and its members were arranged into several well-supported lineages (Fig. 5). The taxa in ST 2 belonged to four sections of West and West (1912), and sections E and I had representatives in both ST 1 and ST 2 (Fig. 5).

A concatenated analysis of only the 21 sequences comprising STAUR + SEB and using a larger number of positions in the data set (2914 nt, for model parameters see Table 2) further raised support for the major lineages in this clade (ST 1 and ST 2; 100% BP and 1.00 PP) and enhanced resolution within the ST 2 subclade but did not increase resolution within ST 1 (results not shown). A shift of *S. capitulatum* from the basal position (Fig. 5, no BP support) to a sister group position with *S. alternans* (55% BP, only in ML) was the only change in internal topology of ST 2. A robust *S. paradoxum/S. polymorphum/S. dispar* clade (87%–98% BP, 1.00 PP) moved to a basal position within ST 2 followed by *S. capitulatum/S. alternans* and a crown clade with four taxa of section E (73%–100% BP, 1.00 PP; results not shown).

The ST 1 and ST 2 subclades differed also in the lengths and the G + C content of their noncoding sequences. Members of ST 1 had consistently lower G + C percentages and shorter 1506 group I intron and ITS2 sequences (400 ± 2.32 nt and 311 ± 2.68 nt, respectively) but longer ITS1 sequences (374 ± 1.9 nt) than the respective sequences in ST 2 (intron, ITS1, and ITS2 were 428 ± 9.6, 368 ± 0.6, and 328 ± 2.3 nt long, respectively).

DISCUSSION

Coding (SSU) and noncoding (1506 group I intron, ITS1, and ITS2) rDNA sequence comparisons were used individually and in combination to analyze phylogenetic relationships between putatively related members of the family Desmidiaceae. Toward this end, we sampled 38 representative taxa from the genera *Staurastrum*, *Staurodesmus*, *Cosmarium*, *Xanthidium*, and *Euastrum* and sequenced a significant part of the rDNA operon. We demonstrate that the four regions of the rDNA operon represent useful phylogenetic markers in the family Desmidiaceae. Despite differences in evolutionary and functional constraints between the coding and noncoding regions, the phylogenies derived from them are largely congruent, and in concatenated analyses the support for most branches increases. The results are largely in conflict with the traditional taxonomy and also contradict anticipated relationships between desmid taxa based on their morphology.

Phylogeny of Staurastrum. In addition to the confirmation of the often stated artificial nature of the genus *Staurastrum*, which is rooted in the extreme morphological diversity of its representative taxa and the lack of well-defined discriminating characters (West and West 1912), our molecular phylogenetic analyses confidently established the monophyletic core of this genus that included most of the species analyzed (the STAUR + SEB clade; Fig. 5). In the present study, four markers consistently united 20 (21 strains) of the 23 *Staurastrum* species studied, representing all morphological types, into a monophyletic assemblage and also resolved to a large extent their phylogenetic relationships. Thus, our data rejected proposals to split the genus into smaller morphologically uniform assemblages (Wille 1890, Palamar-Mordvintceva 1976, 1982) and largely supported its original concept (Ralfs 1848, West and West 1912). Interestingly, the great variability of the genus members in cell shape and size as well as in the pattern of cell wall ornamentation was not reflected in the genetic distance between them as measured by branch lengths, perhaps indicating a rapid and presumably recent radiation. Basically, the STAUR + SEB clade was the shortest branch in each tree, and sequence divergence within it was low compared with other clades and branches. However, sequence divergence was apparently sufficient to resolve a well-supported split within the genus composed of three major lineages.

The original description of *Staurastrum* (Ralfs 1848) characterized its members as being angular (radiate) in apical view and often having processes or spines preferentially at the angles. The only significant reshaping of the genus that somewhat narrowed its concept was made by Teiling (1948), who removed otherwise smooth-celled taxa with a single spine at each angle of a semicell to the newly established genus *Staurodesmus*. Because processes are present in many but by far not all members of the genus *Staurastrum*, angularity is the only character remaining to discriminate its taxa (West and West 1912, Palamar-Mordvintceva 1976). However, homoplasy and infraspecific variability abound, because tri- to multiangular taxa are also known in other desmid genera (Brook 1981) and there is a relatively large group of biradiate *Staurastrum* species (though all its members display processes). Our phylogeny placed taxa with processes (members of the section I, West and West 1912) as basal divergences both in the generic clade (*S. sebaldi*) and in its two subclades (ST 1 and ST 2), whereas species lacking processes (e.g. members of the E-clade; West and West 1912) consistently occupied crown positions in the subclades. This pattern suggests that the ability to form

processes may have been ancestral (plesiomorphic) in the genus and was presumably lost several times independently in the *Staurastrum* lineage. Thus, our phylogeny disproves a hypothetical scenario of morphological evolution in the genus proposed by Fritsch (1953), who considered cosmaroid (lacking processes) forms basal in the genus *Staurastrum*.

Comparison of the morphological properties of taxa retained in *Staurastrum* with those excluded from it reveals another feature that might be of significance to characterize the genus. All 20 taxa comprising the generic clade possess some kind of cell wall ornamentation: granules, warts, or spines distributed more or less regularly on the cell surface. At the same time, two of the three *Staurastrum* species positioned outside the *Staurastrum* clade (*S. orbiculare* and *S. brachiatum*) are smooth celled, and the third taxon, *S. tumidum*, has a cell wall decorated only with a mucro at the lateral angles (a character used by Teiling [1967] to transfer this taxon to the genus *Staurodesmus*). Thus, tentatively, our results suggest that other smooth-celled *Staurastrum* taxa also may not belong to this genus.

The well-resolved internal topology of the *Staurastrum* clade allowed us to test the validity of its divisions and sections (West and West 1912) or subgenera (Turner 1892, Hirano 1959a,b) that are still adopted in some monographic treatments of the genus (Prescott et al. 1982, Croasdale et al. 1994). An analysis of the morphological properties (presence or absence of processes and their position, degree of cell constriction, and pattern of cell wall ornamentation) of the species comprising *Staurastrum* generic clade shows that neither of its subclades could be specifically related to any formal or informal subdivision of the genus. The heterogeneous composition of the subclades suggests that the features previously used to establish divisions/sections within *Staurastrum* have little phylogenetic significance (Nam and Lee 2001).

Each of the three species, *Staurastrum tumidum*, *S. brachiatum*, and *S. orbiculare*, which were significantly positioned outside the genus *Staurastrum*, is distinct in appearance. However, it appears premature to speculate about which features besides the lack of granules/spines on the cell wall might distinguish these taxa from *Staurastrum*. The peculiar nuclear migration during and after morphogenesis in *S. tumidum*, shared with *Xanthidium armatum* (Meindl 1986, Höftberger and Meindl 1993), suggests a possible evolutionary relationship between the two taxa, which is supported by our phylogenetic analyses.

Polyphyly of Staurodesmus. The genera *Staurodesmus* and *Cosmarium* were nonmonophyletic in our analyses, confirming a first assessment based on SSU rDNA sequence comparisons (Gontcharov et al. 2003). In contrast to the previous study in which no significant grouping of *Staurodesmus* taxa was observed, the nine species analyzed here split into three well-supported clades (STD 1, STD 2, and ARTHR; >95% BP, 1.00 PP) and two individual branches (*S. mamillatus* and *S. bulnheimii*). Moreover, two clades, STD 2 and ARTHR, included representatives of other genera, *Staurastrum orbiculare* and *Cosmarium contractum*, respectively, making the genus *Staurodesmus* highly polyphyletic. The only character that differentiates *Staurodesmus* from other genera of the family Desmidiaceae is the presence of a single spine at each angle of a semicell (Teiling 1948, 1967). Before Teiling's work, the main emphasis in the differentiation between *Staurastrum* and *Arthrodesmus* (the major sources of taxa for *Staurodesmus*) was the degree of radiation (tri- to multiradiate in *Staurastrum* vs. exclusively biradiate in *Arthrodesmus*). Teiling concluded that this segregation was artificial because examples of dichotypic (or Janus) forms are frequent in monospinous taxa of both genera and erected a new genus, *Staurodesmus*. Besides the fact that this decision did not solve the equally pronounced contradiction between mono- and plurispinous taxa of the genera *Staurastrum*, *Xanthidium*, and *Arthrodesmus*, rDNA sequence comparisons indicate that the morphological similarity of *Staurodesmus* taxa does not reflect their evolutionary relatedness. Moreover, our results suggest that the concept of the unity of bi- and multiradiate forms, the major point of Teiling's argumentation, may have been mistaken. In the present study, most of the biradiate *Staurodesmus* species analyzed formed a strongly supported ARTHR clade (90%–98% BP, 1.00 PP) distant from other members of the genus. However, *S.* (*Arthrodesmus*) *bulnheimii*, which is also biradiate, was not placed in the ARTHR clade but formed an unresolved individual branch (Fig. 5).

Another challenge to the *Staurodesmus* concept arises from the close relationship between spine-bearing and some smooth-celled species (*Staurastrum orbiculare* in STD 2 and *Cosmarium contractum* in ARTHR). *Staurastrum orbiculare* and *Staurodesmus bieneanus* (which is sometimes treated as a *Staurastrum* species; Coesel 1997, Lenzenweger 1997) both lack spines, whereas the earlier-branching *Staurodesmus mucronatus* displays spines, suggesting that the two later-branching taxa within the STD 2 clade (100% BP, 1.00 PP; Fig. 5) have presumably lost spines during evolution. The situation is less clear with respect to this character (presence/absence of spines) in the ARTHR clade, in which the smooth-celled *Cosmarium contractum* in the concatenated analyses was placed as its basal divergence.

ITS1 and ITS2 secondary structure models. Our putative model of the ITS1 secondary structure generated with the thermodynamic-based folding algorithm revealed six helical domains and a relatively long single-stranded CA-rich region separating the last two helices. Its complexity and relatively high proportion of paired nucleotides contrasts with previous predictions made for its secondary structure in green algae (Coleman et al. 1998), embryophytes (Goertzen et al. 2003), and yeasts (van Nues et al. 1994) in which a major portion of the transcript was said to be single stranded with only a limited number of nucleotides involved in the formation of two to four short stems. The structure agrees, however, with

data presented for abalone (Coleman and Vacquier 2002). The homology of the helices between the Chlorophyta, embryophytes, and Zygnematophyceae remains unclear, and the only obvious feature that links the structure of the ITS1 transcript in these groups is the presence of a CA-rich region that has functional importance for the efficient processing of the spacer (van Nues et al. 1994).

Although thermodynamic-based models may overestimate some secondary structure elements and sequence covariation analysis may be superior in producing more realistic models (Goertzen et al. 2003), the latter approach requires a considerable number of sequences that are presently not available in the Zygnematophyceae. Keeping this in mind, we consider the proposed ITS1 secondary structure model as preliminary but adequate to guide alignments. Comparison of desmid phylogeny based on our ITS1 data set with phylogenies using the other markers (SSU rDNA, 1506 group I intron, and ITS2) reveals no major discrepancies between the topologies and support for clades (the SSU rDNA and ITS1 phylogenies were most similar in this respect).

The secondary structure of the ITS2 transcript in the Desmidiaceae is more representative of ITS2 secondary structures in a wide range of organisms (Hershkowitz and Lewis 1996, Mai and Coleman 1997, Coleman 2003). Typical for these structures is a pyrimidine mismatch pairing at the base of stem II, an AT-rich single-stranded area directly after the stem II, and a string of conserved nucleotides at the 5′ side of helix III that contains a characteristic UGG motif. Not surprisingly, the ITS2 models deduced for the families Desmidiaceae (present study) and Closteriaceae (Denboh et al. 2003), members of the same order Desmidiales, reveal the greatest similarity in overall structure and primary sequence, particularly in the conserved core of the transcript. However, the presence of extensive indels in almost all helices significantly altered their length in these taxa. Whereas in the species studied here helix 1 was the shortest (22–57 nt), in the Closteriaceae it became the longest ($\sim$ 100 nt) helix and displayed a well-conserved additional arm. In contrast, helix II was more than twice as long in most Desmidiaceae compared with the Closteriaceae (59–98 nt vs. 28 nt in *Closterium*). Despite these differences, the basal parts of the first two helices and their flanking spacers are very similar in sequence between the two families.

Our results suggested that the rDNA spacers and intron sequences are rate biased in the order Desmidiales. In the family Closteriaceae, the ITS2 sequences were more conserved compared with the 1506 group I intron and the hypervariable ITS1 (Denboh et al. 2003), whereas an opposite trend was observed in the taxa studied here. It appears that the ITS1 is much less constrained in the fast-evolving genus *Closterium* Nitzsch ex Ralfs (Gontcharov et al. 2003, 2004) than in the Desmidiaceae in which a major part of this spacer is well-alignable between distantly related genera and some regions are almost invariant.

Conclusions. The first application of ribosomal noncoding sequences to address generic concepts of the desmid genera *Staurastrum*, *Staurodesmus*, and *Cosmarium* showed that the 1506 group I intron, ITS1, and ITS2 successfully complemented the conserved SSU rRNA gene and enhanced confidence in the resulting phylogeny. Our phylogenetic analyses confirmed the anticipated polyphyletic nature of the three genera analyzed and revealed significant coding and noncoding sequence divergences among the clades that may be indicative of the presence of several cryptic genera in the family Desmidiaceae. This result demonstrates deficiencies in the currently adopted taxonomic structure of the Desmidiaceae, which is based exclusively on certain morphological characters and begs for its reevaluation.

We thank Annette Coleman (Brown University, RI, USA) for valuable comments on ITS secondary structure models. This study was supported by grants from the Alexander von Humboldt Foundation (V-RKS-1068058), RFBR (05-04-48757a), and FEB RAS to A. A. G.

Bhattacharya, D., Damberger, S., Surek, B. & Melkonian, M. 1996. Primary and secondary structure analysis of the rDNA group I introns of the Zygnematales. *Curr. Genet.* 29:282–6.

Bhattacharya, D., Surek, B., Rüsing, M., Damberger, S. & Melkonian, M. 1994. Group I introns are inherited through common ancestry in the nuclear-encoded rRNA of Zygnematales (Chlorophyta). *Proc. Natl. Acad. Sci. USA* 91:9916–20.

Brook, A. J. 1981. *The Biology of Desmids*. Botanical monographs. 16. Blackwell Science, Boston, Melbourne, 276 pp.

Brook, A. J. 2002. Order Zygnematales. Sub-order Desmidiineae. *In* John, D. M., Whitton, B. A. & Brook, A. J. [Eds.] *The Freshwater Algal Flora of the British Isles—An Identification Guide to Freshwater and Terrestrial Algae*. Cambridge University Press, Cambridge, pp. 530–92.

Cech, T. R. 1988. Conserved sequence and structure of group I introns: building an active site for RNA catalysis—a review. *Gene* 73:259–71.

Coesel, P. F. M. 1997. *De Desmidiaceeën van Nederland. Deel 6 Fam. Desmidiaceae (4)*. Wetenschappelijke Mededeling 220, KNNV Uitgeverij, Utrecht, 95 pp.

Coleman, A. W. 2003. ITS2 is a double-edged tool for eukaryote evolutionary comparisons. *Trends Genet.* 19:370–5.

Coleman, A. W., Preparata, R. M., Mehrotra, B. & Mai, J. C. 1998. Derivation of the secondary structure of the ITS-1 transcript in Volvocales and its taxonomic correlations. *Protist* 149: 135–46.

Coleman, A. W. & Vacquier, V. D. 2002. Exploring the phylogenetic utility of ITS sequences for animals: a test case for abalone (*Haliotis*). *J. Mol. Evol.* 54:246–57.

Croasdale, H. T., Flint, E. A. & Racine, M. M. 1994. *Flora of New Zealand. Freshwater Algae, Chlorophyta, Desmids. III*. Caxton Press, Christchurch, 218 pp.

Denboh, T., Ichimura, T., Hendrayanti, D. & Coleman, A. W. 2003. *Closterium moniliferum-ehrenbergii* (Charophyceae, Chlorophyta) species complex viewed from the 1506 group I intron and ITS2 of nuclear rDNA. *J. Phycol.* 39:960–77.

Felsenstein, J. 1985. Confidence limits on phylogenies: an approach using the bootstrap. *Evolution* 39:783–91.

Fritsch, F. E. 1953. Comparative studies in a polyphyletic group: the Desmidiaceae. *Proc. Linn. Soc. Lond.* 164:258–80.

Galtier, N., Gouy, M. & Gautier, C. 1996. SeaView and Phylo_win, two graphic tools for sequence alignment and molecular phylogeny. *Comput. Applic. Biosci.* 12:543–8.

Gerrath, J. F. 1993. The biology of desmids: a decade of progress. *In* Round, F. E. & Chapman, D. J. [Eds.] *Progress in Phycological Research 9*. Biopress Ltd., Bristol, pp. 79–192.

Gerrath, J. F. 2003. Conjugating green algal & desmids. *In* Wehr, J. D. & Sheath, R. G. [Eds.] *Freshwater Algae of the North America. Ecology and Classification*. Academic Press, San Diego, CA, pp. 353–81.

Goertzen, L. R., Cannone, J. J., Gutell, R. R. & Jansen, R. K. 2003. ITS secondary structure derived from comparative analysis: implications for sequence alignment and phylogeny of the Asteraceae. *Mol. Phylogenet. Evol.* 29:216–34.

Gontcharov, A. A., Marin, B. & Melkonian, M. 2003. Molecular phylogeny of conjugating green algae (Zygnemophyceae, Streptophyta) inferred from SSU rDNA sequence comparisons. *J. Mol. Evol.* 56:89–104.

Gontcharov, A. A., Marin, B. & Melkonian, M. 2004. Are combined analyses better than single gene phylogenies? A case study using SSU rDNA and *rbc*L sequence comparisons in the Zygnematophyceae (Streptophyta). *Mol. Biol. Evol.* 21: 612–24.

Gontcharov, A. A. & Melkonian, M. 2004. Unusual position of the genus *Spirotaenia* (Zygnematophyceae) among streptophytes revealed by SSU rDNA and rbcL sequence comparisons. *Phycologia* 43:105–13.

Hershkovitz, M. A. & Lewis, L. A. 1996. Deep-level diagnostic value of the rDNA-ITS region. *Mol. Biol. Evol.* 13:1276–95.

Hirano, M. 1959a. Flora Desmidiarum Japonicarum. No. 5. *Contrib. Biol. Lab. Kyoto Univ.* 7:226–301.

Hirano, M. 1959b. Flora Desmidiarum Japonicarum. No. 6. *Contrib. Biol. Lab. Kyoto Univ.* 9:302–86.

Hoef-Emden, K., Marin, B. & Melkonian, M. 2002. Nuclear and nucleomorph SSU rDNA phylogeny in the Cryptophyta and the evolution of cryptophyte diversity. *J. Mol. Evol.* 55:161–79.

Höftberger, M. & Meindl, U. 1993. Cell differentiation, ultrastructure and nuclear migration in the desmid *Xanthidium armatum*. *Nova Hedw.* 56:75–88.

Hoshaw, R. W. & McCourt, R. M. 1988. The Zygnemataceae (Chlorophyta): a twenty-year update of research. *Phycologia* 27:511–48.

Huelsenbeck, J. P. & Ronquist, F. 2001. MrBayes: Bayesian inference of phylogenetic trees. *Bioinformatics* 17:754–5.

Joseph, N., Krauskopf, E., Vera, M. I. & Michot, B. 1999. Ribosomal internal transcribed spacer 2 (ITS2) exhibits a common core of secondary structure in vertebrates and yeast. *Nucleic Acids Res.* 27:4533–40.

Kusel-Fetzmann, E. & Schagerl, M. 1992. Verzeichnis der Sammlung von Algen-Kulturen an der Abteilung für Hydrobotanik am Institut für Pflanzenphysiologie der Universität Wien. *Phyton* 32:209–34.

Lenzenweger, R. 1997. *Desmidiaceenflora von Österreich*. Teil 2. J. Cramer, Berlin, Stuttgart, 216 pp.

Mai, J. C. & Coleman, A. W. 1997. The internal transcribed spacer 2 exhibits a common secondary structure in green algae and flowering plants. *J. Mol. Evol.* 44:258–71.

Marin, B., Klingberg, M. & Melkonian, M. 1998. Phylogenetic relationships among the Cryptophyta: analysis of nuclear-encoded SSU rRNA sequences support the monophyly of extant plastid-containing lineages. *Protist* 149:265–76.

Mathews, D. H., Sabina, J., Zuker, M. & Turner, D. H. 1999. Expanded sequence dependence of thermodynamic parameters improves prediction of RNA Secondary Structure. *J. Mol. Biol.* 288:911–40.

McCourt, R. M., Karol, K. G., Bell, J., Helm-Bychowski, K. M., Grajewska, A., Wojciechowski, M. F. & Hoshaw, R. W. 2000. Phylogeny of the conjugating green algae (Zygnemophyceae) based on *rbc*L sequences. *J. Phycol.* 36:747–58.

McFadden, G. I. & Melkonian, M. 1986. Use of Hepes buffer for microalgal culture media and fixation for electron microscopy. *Phycologia* 25:551–7.

Meindl, U. 1986. Autonomous circular and radial motions of the nucleus in *Pleurenterium tumidum* and their relation to cytoskeletal elements and the plasma membrane. *Protoplasma* 135:50–66.

Michel, F. & Westhof, E. 1990. Modeling the three-dimensional architecture of group I catalytic introns based on comparative sequence analyses. *J. Mol. Biol.* 216:585–610.

Nam, M. R. & Lee, O. M. 2001. A comparative study of morphological characters and sequences of rbcL gene in *Staurastrum* of desmid. *Algae* 16:363–7.

Palamar-Mordvintceva, G. M. 1976. Novi rodi Desmidiales. *Ukr. Bot. Zhurn.* 33:396–8.

Palamar-Mordvintceva, G. M. 1982. *Zelenie Vodorosli. Klass Konjugaty. Poriadok Desmidievie. Opredelitel Presnovodnih Vodorosley SSSR*. 11(2). Nauka, Leningrad, 620 pp.

Posada, D. & Crandal, K. A. 1998. Modeltest: testing the model of DNA substitution. *Bioinformatics* 14:817–8.

Prescott, G. W., Bicudo, C. E. & Vinyard, W. C. 1982. *A Synopsis of North American Desmids. Part II. Desmidiaceae: Placodermae*. Section 4. University of Nebraska Press, Lincoln and London, 700 pp.

Prescott, G. W., Croasdale, H. T., Vinyard, W. C. & Bicudo, C. E. M. 1981. *A Synopsis of North American Desmids. Part II. Desmidiaceae*. Section 3. University of Nebraska Press, Lincoln and London, 720 pp.

Ralfs, J. 1848. *The British Desmidieae*. Reeve, Benham and Reeve, London, 226 pp.

Surek, B. & Melkonian, M. 2004. CCAC—culture collection of algae at the University of Cologne: a new collection of axenic algae with emphasis on flagellates. *Nova Hedw.* 79:77–91.

Surek, B. & Sengbusch, P. 1981. The localization of galactosyl residues and lectin receptors in the mucilage and the cell walls of *Cosmocladium saxonicum* (Desmidiaceae) by means of fluorescent probes. *Protoplasma* 108:149–61.

Swofford, D. L. 2002. *PAUP* Phylogenetic Analysis Using Parsimony (And Other Methods)*. Beta version 10. Sinauer Associates, Sunderland, MA.

Teiling, E. 1948. *Staurodesmus*, genus novum-containing monospinous desmids. *Bot. Not.* 1948:49–83.

Teiling, E. 1954. *Actinotaenium*, genus Desmidiacearum resuscitatum. *Bot. Not.* 107:376–426.

Teiling, E. 1967. The desmid genus *Staurodesmus*. *Ark. Bot. Ser.* 2:6:467–629.

Turner, W. B. 1892. Algae aquae dulcis Indiae orientalis. The freshwater algae (principally Desmisieae) of East India. *Kongl. Svenska. Vet. Akad. Handl.* 25:1–187.

van Nues, R. W., Rientjes, J. M. J., van Dersande, C. A. F. M., Zerp, S. F., Sluiter, C., Venema, J., Planta, R. J. & Raue H, . A. 1994. Separate structural elements within internal transcribed spacer-1 of *Saccharomyces cerevisiae* precursor ribosomal RNA direct the formation of 17S and 26S ribosomal RNA. *Nucleic Acids Res.* 22:912–9.

West, W. & West, G. S. 1912. *A Monograph of the British Desmidiaceae*. Vol. 4. Ray Society, London, 191 pp.

Wille, N. 1890. Desmidiaceae. *In* Engler, A. & Prantl, E. [Eds.] *Die Natürlichen Pflazenfamilien*. I. 2. W. Engelmann, Leipzig, 1–16 pp.

Woese, C. R., Winker, S. & Gutell, R. R. 1990. Architecture of ribosomal RNA: constrains on the sequence of "tetra-loops". *Proc. Natl. Acad. Sci. USA* 87:8467–71.

Wuyts, J., De Rijk, P., Van de Peer, Y., Pison, G., Rousseeuw, P. & De Wachter, R. 2000. Comparative analysis of more than 3000 sequences reveals the existence of two pseudoknots in area V4 of eukaryotic small subunit ribosomal RNA. *Nucleic Acids Res.* 28:4698–708.

Wuyts, J., Van de Peer, Y. & De Wachter, R. 2001. Distribution of substitution rates and location of insertion sites in the tertiary structure of ribosomal RNA. *Nucleic Acids Res.* 29:5017–28.

Zuker, M. 2003. Mfold web server for nucleic acid folding and hybridization prediction. *Nucleic Acids Res.* 31:3406–15.